Surface Charge-Switching Polymeric Nanoparticles for Bacterial Cell Wall-Targeted Delivery of Antibiotics

Aleksandar F. Radovic-Moreno[†,‡], **Timothy K. Lu**[#], **Vlad A. Puscasu**[‡], **Chris J. Yoon**[‡,#], **Robert Langer**[†,‡,*], and **Omid C. Farokhzad**[¶,*]

[†]Harvard-MIT Division of Health Sciences & Technology, Cambridge, MA 02139

[‡]Department of Chemical Engineering, Massachusetts Institute of Technology, Cambridge, MA 02139

[#]Synthetic Biology Group, Department of Electrical Engineering & Computer Science, Massachusetts Institute of Technology, Cambridge, MA 02139

[¶]Laboratory of Nanomedicine and Biomaterials, Department of Anesthesiology, Brigham & Women's Hospital, Harvard Medical School, Boston, MA 02115

Abstract

Bacteria have shown a remarkable ability to overcome drug therapy if there is a failure to achieve sustained bactericidal concentration or if there is a reduction in activity *in situ*. The latter can be caused by localized acidity, a phenomenon that can occur as a result of the combined actions of bacterial metabolism and the host immune response. Nanoparticles (NP) have shown promise in treating bacterial infections, but a significant challenge has been to develop antibacterial NPs that may be suitable for systemic administration. Herein we develop drug-encapsulated, pH-responsive, surface charge-switching poly(D, L-lactic-co-glycolic acid)-*b*-poly(L-histidine)-*b*-poly(ethylene glycol) (PLGA-PLH-PEG) nanoparticles for treating bacterial infections. These NP drug carriers are designed to shield nontarget interactions at pH 7.4 but bind avidly to bacteria in acidity, delivering drugs and mitigating in part the loss of drug activity with declining pH. The mechanism involves pH-sensitive NP surface charge-switching, which is achieved by selective protonation of the imidazole groups of PLH at low pH. NP binding studies demonstrate pH-sensitive NP binding to bacteria with a 3.5±0.2 to 5.8±0.1 fold increase in binding to bacteria at pH 6.0 compared to 7.4. Further, PLGA-PLH-PEG-encapsulated vancomycin demonstrates reduced loss of efficacy at low pH, with an increase in minimum inhibitory concentration of 1.3-fold as compared to 2.0-fold and 2.3-fold for free- and PLGA-PEG-encapsulated vancomycin, respectively. The PLGA-PLH-PEG NPs described herein are a first step towards developing systemically administered drug carriers that can target and potentially treat Gram-positive, Gram-negative, or polymicrobial infections associated with acidity.

Keywords

[*]To whom correspondence may be addressed. rlanger@mit.edu, ofarokhzad@zeus.bwh.harvard.edu.

In recent years, advances in the design of nanoparticles (NPs) for drug delivery applications have enabled potential strategies for improving the treatment of a variety of diseases.[1-3] So far, success has been linked to the ability to precisely engineer interactions between NPs and the biologic milieu in ways that may lead to gains in drug potency or properties *in vivo*. Promising methods include: molecular targeting,[4, 5] environmental sensing leading to NP property switching or drug release,[6-8] optimizing NP physicochemical properties,[9, 10] and sustained drug release.[11, 12] Despite these advances, NPs have only really begun to demonstrate their potential in treating infections. Recent reports have demonstrated advances in selective targeting of bacterial membranes for lysis,[13] improved drug delivery,[14, 15] enhanced drug function,[16-18] and the potential for selective accumulation at sites of infection due to increased vascular permeability.[19] In particular, designing methods for improving antibiotic targeting and activity *in vivo*, such as through NP drug carrier design, are important efforts that may: 1) improve treatment outcomes with fewer side effects, 2) reduce the likelihood of drug resistance emerging given that ineffective drug dosing or targeting can lead to the rapid development of drug resistance under inauspicious conditions,[20] and 3) overwhelm drug resistance mechanisms with high sustained local drug concentrations.[3, 21, 22] However, a significant challenge has been designing antibacterial NPs that may be suitable for systemic administration. A common feature of antibacterial NPs developed to date is a strong, relatively pH-insensitive cationic surface charge which, while demonstrating potent bactericidal activity *in vitro*,[23, 24] is not specific for bacteria and is known in some cases to adversely affect the blood circulation and biodistribution properties of NPs[25] and potentially demonstrating toxicity.[26] The ability to systemically administer antibacterial NP formulations may enable their use in a variety of applications, including examples where infections are disseminated, where local delivery would be overly complicated or impossible, or where other delivery routes or methods are either compromised by disease pathology or ineffective.

Bacteria are highly adaptive organisms that have evolved the ability to thrive in various types of environments. Of these environments, low pH is particularly significant both because of its association with serious infections and its implications for treatment. Certain antibiotics are known to demonstrate significant loss of activity in acidity,[27] and even more troubling, a reduction in localized pH is usually a sequela of worsening disease severity and prognosis – precisely when maximal efficacy is most needed.[28] Bacteria may habitat acidic environments in the body either because acidity is the naturally prevailing condition, such as the stomach (pH 1.0-2.0), intestines (pH 5.0-8.0), vagina (pH 4.0-5.0), bladder (pH 4.5-8.0), and skin (pH 4.0-5.5)[29, 30] or through a combination of bacterial activity and the resulting immune response. Acidity associated with infections occurs through a combination of low oxygen tension triggering anaerobic fermentation in certain bacteria, the products of which are organic acids including lactic, and acetic acids[31] and through inflammation, which is known to exacerbate acidity due to increased levels of acidic products through mechanisms including production of lactic acid during phagocytosis.[32, 33] Together, these factors are associated with reducing the pH of a site of infection as far as pH 5.5.[34, 35] Examples of clinical indications where pH-dependent loss of drug activity may be relevant include pneumonias, especially in cystic fibrosis (CF) patients,[36, 37] abscesses,[34] and *H. pylori* infections, the major cause of peptic ulcers.[38] Developing systemically available NP drug carriers that can target and improve antibiotic properties in the setting of localized acidity may therefore be a method to improve treatment of these and potentially other infections.

In the present work, we sought to develop a polymeric NP antibiotic carrier that could target the cell walls of bacteria in acidity in order to potentially improve bacterial targeting and antibiotic properties at sites of infections. We chose to target the cell wall because its integrity is vital to bacterial survival, it is the outermost and therefore most accessible layer, and is the site of action of many antibiotics. Important design criteria to achieve effective

cell wall targeting NPs are the following. First, a targeting strategy that applies across a range of bacterial classifications is important, since many serious infections are polymicrobial and acidity is not isolated to one particular type of bacterium. For example, 67% of CF patients test positive for *S. aureus* (Gram-positive), and 51% with *P. aeruginosa* (Gram-negative) in their sputum, with co-infection having an additive effect on disease pathology.[39] To achieve this broad NP bacterial targeting, we chose to exploit electrostatic attractions, since many different types of bacteria are known to be negatively charged due to the composition of their cell walls,[40] and this approach has been validated extensively on surfaces,[41] using cationic Eudragit/PLGA[42] or chitosan[23] NPs, as well as by noting that electrostatics, at least partially, underlie the binding mechanism of scores of antimicrobial peptides and cationic peptide-based NPs.[43, 44] Second, selecting an encapsulation strategy that can be used with a diversity of agents is key, as bacterial drug susceptibility is constantly evolving and new agents are continuously being developed. We selected PLGA as the basis for an encapsulation matrix because it offers the advantages of low toxicity, flexibility in terms of drug payload, ease of synthesis, and the ability to fine tune surface properties through NP engineering.[3] In addition, PLGA has been validated as an effective antibiotic-laden implant or microparticle formulation for antibiotics, and, when formulated into NPs, has demonstrated extended[45, 46] and optimized[11] release kinetics or improved efficacy.[18] Third, the potential to achieve infection-specfic targeting through a combination of extended circulation time and low non-specific binding in the blood but avid bacterial binding when located in acidity-associated infections was desirable to improve systemic administration potential. NPs have the potential to target areas of infection due to localized increases in vascular permeability mediated by both the cell-mediated inflammatory response as well as by direct activation of the kinin-kallikrein system by bacterial proteases, though this mechanism has not been deeply investigated in this context.[19] Nevertheless, it is clear that plain PLGA NPs would have a limited ability to exploit this potential targeting mechanism due to their rapid clearance (in seconds to minutes) by the mononuclear phagocytic system.[47] Surface modifying PLGA NPs with PEG is widely known to reduce non specific interactions, leading to prolonged circulation, but PLGA-PEG NPs alone lack significant bacterial binding ability and therefore would be expected to drain through the (intact) lymphatics at infection sites. We sought to maximize the potential for infection-specfic targeting by minimizing nontarget interactions at physiologic pH 7.4 and by using acidity as a trigger to selectively produce a cationic NP surface for binding. To impart this pH functionality, we incorporated poly-L-histidine, a peptide containing imidazole groups that gain protons under acidic conditions (pKa ~6.0-6.5) into a triblock copolymer structure consisting of poly(D, L-lactic-co-glycolic acid)-*b*-poly(L-histidine)-*b*-poly(ethylene glycol) (PLGA-PLH-PEG), which could be formulated into NPs using emulsion/solvent evaporation techniques. Under acidic conditions, the PLH segment would become positively charged, yielding an overall positive zeta potential on the NP surface, facilitating interactions with the negatively charged elements of bacterial cell wall and producing strong multivalent electrostatic-mediated binding. Finally, it was important to be able to demonstrate efficacy with a clinically significant antibiotic. We chose the glycopeptide antibiotic vancomycin because of its established role in treating serious and life threatening infections, because it loses activity at low pH, because it has a low minimum inhibitory concentration (MIC), and because its targets are components of the cell wall. The results of our studies demonstrate that pH-sensitive, surface charge-switching PLGA-PLH-PEG NPs can be used to bind to bacteria under conditions of acidity. Further, when NPs are used to encapsulate vancomycin, vancomycin demonstrates a higher MIC than free drug but a partial reduction in its loss of activity in acidity as compared to free drug and non-pH sensitive PLGA-PEG delivery systems. This work is a first step towards developing systemically-delivered bacteria-targeting NP drug delivery systems and may have implications for designing improved treatment strategies for various acidity-associated infections.

RESULTS AND DISCUSSION

Design of Surface Charge-Switching PLGA-PLH-PEG NPs

A linear PLGA-PLH-PEG architecture was selected to provide NP characteristics compatible with extended circulation, charge-mediated targeting, and controlled drug release (Figure 1). PLGA was used to form the hydrophobic core and drug depot. To decide how to incorporate the PLH in the NPs, we reasoned that by placing the PLH between the PLGA and PEG blocks to yield the linear structure PLGA-PLH-PEG we could achieve the following: 1) the PLGA segment could form a solid core matrix without having the destabilizing force of PLH at acidic pH, since PLLA-PEG / PLH-PEG mixed micelles have been demonstrated to be effective pH-sensitive triggered-release systems.[48, 49] We wanted to retain the slow release characteristics of intact NPs in order to reduce complexity in processing and use, potentially achieve a larger area-under-the-curve (AUC) at the site of infection, and be able tailor drug-bacterium interactions using NPs. 2) PLH would be preferentially placed near the NP surface as the polymer self-assembled, due to its intrinsic hydrophilicity under typical formulation conditions as well as its close association with the PEG, which would preferentially rise to the surface due to its relative hydrophilicity. This is significant in that it would increase the magnitude of the surface charge switching capability, as the cationic charge of the PLH at acidic pH would be closer to the NP surface. 3) Having the PEG portion at the distal end of the polymer would facilitate NP colloidal stability and circulation time at physiologic pH, as has been reported in the literature.[47] The polymer was synthesized using an block end-grafting strategy (see Materials and Methods).

NP Formulation and pH-Dependent Characterization

Understanding the physicochemical properties of PLGA-PLH-PEG NPs as a function of pH was key to tailoring NP-bacterium interactions. To evaluate these properties, we formulated PLGA-PLH-PEG and PLGA-PEG polymers into nanoparticles using a modified double emulsion/solvent evaporation method.[50] The NPs were purified by triple ultrafiltration, resuspended in appropriate pH-buffered PBS solutions ranging from pH 5.5 to pH 7.4, and characterized in terms of their physicochemical properties by quasi-elastic laser light scattering. The results show that the PLGA-PLH-PEG NPs switched their surface charge from a negative zeta potential at pH 7.4 (ζ = −3.9±0.4 mV, N=3) to a positive one with reduction in pH, with the transition occurring as early as pH 7.0 (ζ = 2.3±1.0, N=3) (Figure 2A) and a linear slope of −8.6 mV/pH unit (R^2 = 0.951). In contrast, PLGA-PEG diblock copolymer had a negative zeta potential at every pH tested (At pH 7.4, PLGA-PEG ζ = −36.5±0.5 mV, N=3) and demonstrated little pH sensitivity, with a slope of −2.9 mV/pH unit (R^2 = 0.447). The lower R^2 reflects the observation that subtle changes only occurred at a very low pH of 5.5. The negative charge of both polymers at pH 7.4 is likely a result of residual negative charge from acid groups in the PLGA-COOH precursor, partially hydrolyzed PLGA chains, and from carbonyl groups in the PLGA block. The more positive zeta potential of the PLGA-PLH-PEG relative to PLGA-PEG is likely due to the presence of the neutrally charged PLH block near the surface. The gain in charge with reduction in pH is due to the exponentially increasing presence of positive charges from the imidazole group of the PLH with reductions in pH, as described by the Henderson-Hasselbach equation. Both PLGA-PLH-PEG (mean size = 196.0±7.8 nm, N=3) and PLGA-PEG (mean size = 222.1±1.8 nm, N=3) NPs did not demonstrate large differences in size with decreasing pH (Figure 2B). In addition, transmission electron microscopy (TEM) suggests that the PLGA-PLH-PEG NPs retained their integrity at acidic pH values (Figure 2C), in contrast to reports of PLLA-PEG / PLH-PEG mixed micelles.[49]

pH-Dependent Binding of NPs to Bacteria

We then evaluated whether the observed changes in NP physicochemical properties with pH would enable binding to bacteria under acidic conditions. As model organisms of two major subtypes of bacteria, we selected the Gram-negative *Escherichia coli* (*E. coli*) and Gram-positive *Staphylococcus aureus* (*S. aureus*). We initially evaluated to what extent PLGA-PLH-PEG NPs could bind to these bacteria as a function of pH by labeling NPs using Alexa-488 to form green fluorescent NP-488 (modified with Alexa-488 PLGA, see Materials and Methods section) and incubating them with the different bacteria for 30 min in pH-adjusted PBS solutions from pH 5.5 to 7.4 at 37°C. PLGA-PEG NP-488 were used as a non-pH-sensitive control. Following binding, the NP-488-bacteria aggregates and/or bacteria were centrifuged and washed, resuspended in PBS pH 7.4, and run on a flow cytometer to evaluate their fluorescence levels. In the case of both bacteria, a large and significant ($p < 0.05$) increase in binding was observed as pH was decreased < pH 6.5 (Figure 3A, 3B). The increase in binding to both *S. aureus* and *E. coli* became very pronounced at pH 6.0 (*S. aureus* PLGA-PLH-PEG 3.5±0.2; *E. coli* 5.8±0.1, all N=3) as compared to PLGA-PEG (*S. aureus* 1.0±0.1; *E. coli* 1.1±0.1, all N=3) and peaked at pH 5.5. Given that NP residence time at a site of infection may be limited, we wished to determine how quickly NPs bound to bacteria under acidic conditions. We performed a kinetic study of PLGA-PLH-PEG NPs to both types of bacteria at pH 6.0, selecting incubation time points between 10 min and 4 hours and measuring bacteria-associated fluorescence using flow cytometry. We observed rapid saturation of fluorescence, with ~80% of maximal binding occurring within 10 minutes for both *E. coli* (Figure 3C) and *S. aureus* (Figure 3D). This binding kinetics data suggests that even a relatively short residence time at an acidic site of infection might be sufficient to enable binding to bacteria using PLGA-PLH-PEG NPs. To provide visual confirmation of PLGA-PLH-PEG NP binding to bacteria, we used fluorescence confocal microscopy. PLGA-PLH-PEG NP-488 were freshly prepared, purified, and resuspended in pH 6.0 or pH 7.4 PBS solutions. *S. aureus* bacteria were prepared as before and inoculated into the PLGA-PLH-PEG NP-488-containing solutions. We selected *S. aureus* as a model bacterium for the confocal studies due to our observation of the slightly more positive but still anionic charge of these bacteria as compared to *E. coli*, which would therefore yield a more conservative confirmation of our flow cytometry-based results. The NP-488/bacteria suspension was placed in an incubated shaker at 37°C for 30 min to allow NP-488 binding to bacteria. After washing unbound NP-488s by centrifugation with repeated PBS pH 7.4 buffer washes, bacteria were stained using *Bac*Light™ Red, a commercially available small molecule that binds to bacteria, according to manufacturer instructions. Confocal microscopy visually confirmed the pH-sensitive nature of PLGA-PLH-PEG NP-488 binding to bacteria (Figure 4). Close inspection (Figure 4E, 4F) demonstrates that strong fluorescence can be seen at the bacterial cell wall in the pH 6.0 NP-488 treated but not pH 7.4 NP-488 treated group. No NP-488 fluorescence can be observed in the interior of the bacteria, suggesting that PLGA-PLH-PEG NPs are unable to penetrate the cell wall, which was expected given the formidable diffusion barriers presented. In addition, after pH 6.0 NP-488 treatment, one can observe that the NP-488s have triggered agglutination of bacteria into larger aggregates as compared to what is observed with pH 7.4 NP-488 bacteria. This may be due to the positively charged NP-488s bridging two negatively charged bacteria together in the pH 6.0 NP-488 but not pH 7.4 NP-488 group.

Antimicrobial Studies

Finally, we were interested in seeing whether PLGA-PLH-PEG NP binding to the bacterial surface had an impact on antibiotic efficacy, and how this compared to PLGA-PEG NP and free drug formulations. As a proof-of-concept, we chose to examine *S. aureus* susceptibility to formulations of vancomycin, a glycopeptide antibiotic used clinically to treat infections

involving *S. aureus*, particularly drug resistant strains. Vancomycin was encapsulated in NPs, washed, and resuspended in pH 6.0 or pH 7.4 PBS. Encapsulation efficiency PLGA-PLH-PEG (42.2±8.1%, N=3), PLGA-PEG (39.2±1.4%, N=3) and drug loading PLGA-PLH-PEG (7.8±1.6%, N=3), PLGA-PEG (7.3±0.3%, N=3) were evaluated. The minimum inhibitory concentration (MIC) of PLGA-PLH-PEG NP formulated vancomycin (PLGA-PLH-PEG[Vanco]), PLGA-PEG NP formulated vancomycin (PLGA-PEG[Vanco]), and free vancomycin were determined using the microplate dilution method at pH 6.0 or pH 7.4 (Figure 5). The minimum bactericidal concentrations were determined semi-quantitatively by subculturing to antibiotic-free TSB agar plates. For the NP formulations of vancomycin, the vancomycin concentration is reported as the total concentration of vancomycin in the NP at the beginning of treatment. Vancomycin is released from the NP at a steady rate over a 50 hour period (see SI), which is consistent with many studies of drug release from NPs. We reasoned that the initial vancomycin concentration inside the NPs was both the most conservative and useful measure of NP antibiotic formulation efficacy. The results show (Figure 5, Table 1) that at pH 7.4, free vancomycin is the most potent formulation of the drug (MIC 1.2±0.6 ug/mL, MBC 3.1 ug/mL, N=3), but that this is strongly pH sensitive. At pH 6.0, free vancomycin loses potency by a factor of 2.0, consistent with other observations[27] (Figure 5). PLGA-PEG NP vancomycin formulations required higher initial vancomycin concentration than free drug to achieve antibacterial effects at physiologic pH 7.4 (MIC 6.0±0.7 ug/mL, MBC 20. ug/mL, N=4), and similarly demonstrated significant pH sensitive loss in activity by a factor of 2.3 (MIC 14.2±1.9 ug/mL, MBC 40. ug/mL, N=4). As expected, PLGA-PLH-PEG NP formulations of vancomycin behaved similar to PLGA-PEG NP formulations at pH 7.4 (MIC 6.8±2.1 ug/mL, MBC 20. ug/mL, N=4, p=0.54) but had significantly improved activity at pH 6.0, demonstrating less loss in activity with pH, by a factor of 1.3 (MIC 8.6±0.5 ug/mL, MBC 20. ug/mL, N=4, $p < 0.05$) (Figure 5). Further, this suggests that promoting NP-bacterium interactions under acidic conditions, such as was demonstrated, can partially mitigate the loss of activity with pH, further highlighting the potential of this delivery system for treating infections associated with localized acidity.

Summary

We have developed a pH-responsive, surface charge-switching polymeric nanoparticle drug delivery system for targeting bacterial cell walls at sites of acidic infections. We demonstrate that pH-sensitive PLGA-PLH-PEG NPs rapidly (~80% of maximum within 10 min) bind to both Gram-positive (*S. aureus*) and Gram-negative (*E. coli*) organisms under acidic conditions and that increased binding can be correlated to sharp increases in NP zeta potential with reductions in pH. Further, we demonstrate that vancomycin encapsulated in PLGA-PLH-PEG NPs demonstrates a 1.3-fold pH-dependent increase in MIC against *S. aureus*, an improvement over free vancomycin and PLGA-PEG vancomycin, which demonstrate 2.0 and 2.3 fold increase at pH 6.0, respectively. The proof-of-concept *in vitro* studies described in this work may – pending the results of further extensive *in vitro* and *in vivo* evaluation – be applied to an array of clinical conditions in which systemic delivery approaches are desirable, where localized acidity occurs, and where antibiotic efficacy is affected by acidity, potentially suggesting methods of improving drug targeting and efficacy in these infections. Future work in this area should first explore to what extent bacterial cell wall targeting using a surface charge-switching mechanism can lead to both prolonged circulation and effective targeting as compared to untargeted NPs and free drugs *in vivo*. The pH-sensitive, surface-charge switching PLGA-PLH-PEG NPs, while potentially improving the binding specificity for bacterial cell walls as compared to pH-insensitive cationc NPs delivered systemically, still use non-specific charge-charge interactions to mediate binding locally at the site of infection. Sites of infection are populated with negatively charged tissue cells, which will not only compete with the bacteria for the positively charged NPs, but also have the ability to internalize and sequester the NPs,

preventing them from interacting with the bacteria. Therefore, exploring to what extent competition between bacteria and tissue cells at a site of infection for the charged NPs affects both bacterial targeting and antibiotic delivery will be important. Future studies should also: 1) compare the efficacy of antibiotics delivered using these groups *in vivo*, 2) investigate methods of improving the potency of NP-vancomycin formulations, and 3) explore the growth inhibition potential in Gram-negative infections.

MATERIALS AND METHODS

Polymer Synthesis and Characterization

We synthesized the triblock copolymer poly(D, L-lactic-co-glycolic acid)-*b*-poly(L-histidine)-*b*-poly(ethylene glycol) (PLGA-PLH-PEG) using a polymer end grafting strategy (see SI for details). In brief, PLH was custom synthesized to contain 20 or 30 repeats of L-histidine with an N-terminal lysine and a C-terminal cysteine to facilitate conjugation reactions. First, PLH-SH and orthopyridyl disulfide (OPSS) modified PEG blocks were reacted to form a diblock copolymer using thiol-to-orthopyridyldisulfide chemistry and purified by dialysis and lyophilization. The PLGA was conjugated to the NH_2-PLH-PEG diblock copolymer using EDC/NHS carbodiimide chemistry and purified by precipitation. The reaction products and intermediates were characterized by MALDI-TOF, GPC, and ^{1}H-NMR.

NP Formulation

NPs were formulated (PLGA-PLH-PEG or PLGA-PEG in the same manner) using modified emulsion/solvent evaporation techniques (see SI for details). In brief, a typical vancomycin-containing NP formulation was prepared by sonicating 50 uL of a 4 g/L solution of vancomycin hydrochloride (Sigma Aldrich, St. Louis, MO) into 500 uL ethyl acetate containing 2 g/L polymer. This primary emulsion was sonicated into 2 mL 10% w/v NaCl solution to form the W/O/W double emulsion, diluted into 8 mL 5% w/v NaCl, and solvent allowed to evaporate for 4 hours prior to purification using ultrafiltration. To form green fluorescent NPs, Alexa-488-modified PLGA was blended into the organic phase at 15% w/w total polymer and no salt or vancomycin were used in the emulsion process.

Drug Encapsulation and Release Studies

2.0 mg of PLGA-PEG or PLGA-PLH$_{30}$-PEG NPs were formulated with 0.4 mg initial vancomycin. Drug encapsulation was determined by quantifying the amount of unencapsulated drug relative to the initial amount of drug by UV absorbance at 220 nm relative to a standard curve. Drug release was conducted by suspending NPs in 4 mL of pH-adjusted PBS (6.0 or 7.4), separating NPs and free drug by ultrafiltration, and quantifying free drug at each time point in triplicate.

pH-Dependent Physicochemical Property Characterization

ZetaPALS analysis—NPs made with different PLH lengths were prepared without vancomycin, purified, and resuspended in pH-adjusted PBS solution in triplicate. Similarly, bacteria were centrifuged, washed, and resuspended in pH-adjusted PBS solutions. Size and zeta potential were measured for each solution by quasi-elastic laser light scattering using a ZetaPALS dynamic light scattering detector (15 mW laser, incident beam 676 nm, Brookhaven Instrument Corporation).

Transmission Electron Microscopy—PLGA-PLH$_{20}$-PEG NPs were prepared, washed to remove residual organic solvent, resuspended at 5 mg/mL in a 1% w/v uranyl acetate

solution (pH ~5.5), deposited onto carbon supported copper TEM grids for 5 min, dried, then imaged on a JEOL 200 CX TEM (MIT CMSE) at an accelerating voltage of 200 kV.

Nanoparticle-Bacterium Binding Studies

Bacterial Culture—*Escherichia coli* (ATCC# 11229) were cultured in LB broth (BD# 244620). Colonies were streaked on an LB-agar plate, selected, inoculated into 5 mL of growth medium and allowed to grow overnight in an incubated shaker at 37°C. *Staphylococcus aureus* (ATCC# 25923) were cultured in similar fashion using Tryptic Soy Broth (TSB, BD#211825).

Flow Cytometry NP-488 Binding Assays—PLGA-PLH$_{20}$-PEG and PLGA-PEG NP-488s were prepared, purified, and concentrated into 100 uL of pure water. Bacteria were overgrown overnight in 5 mL of growth medium, spun down, washed in saline solution, then resuspended in PBS previously pH-adjusted to 5.5, 6.0, 6.5, 7.0, or 7.4 using a dilute aqueous HCl solution. NP-488 were added to the bacteria and incubated for 30 minutes. For binding kinetic studies, time points ranged from 10 minutes to 4 hours. After incubation was complete, bacteria were spun down, unbound NP-488 in the supernatant were removed, bacteria were resuspended in PBS pH 7.4, and run on a flow cytometer (FACSCalibur, BD Biosciences, Koch Institute Flow Cytometry Core). Forward scatter (FSC), side scatter (SSC), green fluorescence (ex: 488, filter: 530/30), and red fluorescence (ex: 488, filter: 650 LP) data were collected on a minimum of 10,000 events per sample. Bacteria were gated for live using FSC vs SSC plots using an untreated negative control for reference.

Fluorescence Confocal Imaging—Overnight overgrown cultures of *S. aureus* were spun down at 3,000 RCF for 5 min. A 1:10 dilution of the bacteria in PBS was washed in saline solution then resuspended in 500 uL PBS pH-adjusted to pH 6.0 or pH 7.4 using dilute HCl solution. Freshly prepared PLGA-PLH$_{20}$-PEG NP-488 were prepared, purified, resuspended in a small volume of sterile water, then diluted into the bacterial pH-buffered suspension. The bacteria and NP-488 were placed in an incubated shaker for 30 min at 37°C to allow NP-488 binding to occur. At the 30 minute time point, the suspension was centrifuged at 3,000 RCF for 5 min to pellet bacteria and bacteria-NP-488 aggregates. The pellet was washed 3x in PBS pH 7.4 and resuspended in 100 uL of PBS pH 7.4. Bacteria were stained using *Bac*Light™ Red (Life Technologies #B-35001, Carlsbad, CA) for 30 min following the manufacturer's protocol, placed on a glass slide, coverslipped, then taken immediately for fluorescent laser scanning confocal imaging (Zeiss LSM 510 meta, W. M. Keck Microscopy Facility, Whitehead Institute at MIT). Excitation lasers used: 488 nm for green channel, 543 nm for red channel.

Antibacterial Studies

Minimum Inhibitory Concentration (MIC)—The MIC of the different vancomycin formulations against *S. aureus* were determined using the microplate broth dilution method. Briefly, *S. aureus* from overnight cultures were inoculated into 5 mL TSB and allowed to enter log phase (OD$_{600}$ ~0.3) after approximately 2 hours of incubation. NPs (PLGA-PLH$_{30}$-PEG or PLGA-PEG) encapsulating vancomycin were freshly prepared, purified, and serially diluted into a final volume of 100 uL of sterile water in triplicate at a 2x concentration in clear, flat bottom 96 well plates. Bacteria in log phase were diluted to a theoretical OD$_{600}$ of 0.001 in either TSB pH adjusted to pH 7.4 or pH 6.0 using a dilute sterile HCl solution and seeded onto the microplates to produce a final volume per well of 200 uL. The OD$_{600}$ was measured immediately before placing into an incubated shaker at 37°C, 18 hours later. The drug concentration is the total drug concentration present inside the nanoparticles, as determined by encapsulation efficiency and drug release studies. The MIC was determined as suggested by Lambert and Pearson[51] by fitting Gompertz functions

to bacterial growth data using least squares regression techniques. No change in pH with time was detected.

Minimum Bactericidal Concentration (MBC)—The MBC was determined by plating bacterial inoculum from the MIC studies onto antibiotic-free TSB agar plates. The MBC was reported as the smallest concentration that results in no visible bacterial growth within 24 hours.

Statistics

All data are expressed as mean ± SD. Differences between groups were assessed using one-way ANOVA (comparisons of vancomycin formulation efficacy were performed on MIC data only). Post hoc group comparisons were done using Fisher's LSD method. Least squares regressions were used to fit Gompertz functions to bacterial growth inhibition data. A significance level of $p < 0.05$ was used for all comparisons.

Supplementary Material

Refer to Web version on PubMed Central for supplementary material.

Acknowledgments

REFERENCES

1. Lobatto ME, Fuster V, Fayad ZA, Mulder WJ. Perspectives and Opportunities for Nanomedicine in the Management of Atherosclerosis. Nat Rev Drug Discov. 2011; 10:835–852. [PubMed: 22015921]

2. Peer D, Karp JM, Hong S, Farokhzad OC, Margalit R, Langer R. Nanocarriers As an Emerging Platform for Cancer Therapy. Nat Nanotechnol. 2007; 2:751–760. [PubMed: 18654426]

3. Zhang L, Pornpattananangku D, Hu CM, Huang CM. Development of Nanoparticles for Antimicrobial Drug Delivery. Curr Med Chem. 2010; 17:585–594. [PubMed: 20015030]

4. Gu F, Zhang L, Teply BA, Mann N, Wang A, Radovic Moreno AF, Langer R, Farokhzad OC. Precise Engineering of Targeted Nanoparticles by Using Self-Assembled Biointegrated Block Copolymers. Proc Natl Acad Sci U S A. 2008; 105:2586–2591. [PubMed: 18272481]

5. Hu-Lieskovan S, Heidel JD, Bartlett DW, Davis ME, Triche TJ. Sequence-Specific Knockdown of EWS-FLI1 by Targeted, Nonviral Delivery of Small Interfering RNA Inhibits Tumor Growth in a Murine Model of Metastatic Ewing's Sarcoma. Cancer Research. 2005; 65:8984–8992. [PubMed: 16204072]

6. von Maltzahn G, Park JH, Lin KY, Singh N, Schwoppe C, Mesters R, Berdel WE, Ruoslahti E, Sailor MJ, Bhatia SN. Nanoparticles that Communicate *In Vivo* to Amplify Tumour Targeting. Nat Mater. 2011; 10:545–552. [PubMed: 21685903]

7. Poon Z, Chang D, Zhao X, Hammond PT. Layer-by-Layer Nanoparticles with a pH-Sheddable Layer for *In Vivo* Targeting of Tumor Hypoxia. ACS Nano. 2011; 5:4284–4292. [PubMed: 21513353]

8. Pornpattananangkul D, Zhang L, Olson S, Aryal S, Obonyo M, Vecchio K, Huang CM. Bacterial Toxin-Triggered Drug Release from Gold Nanoparticle-Stabilized Liposomes for the Treatment of Bacterial Infection. J Am Chem Soc. 2011; 133:4132–4139. [PubMed: 21344925]

9. Petros RA, DeSimone JM. Strategies in the Design of Nanoparticles for Therapeutic Applications. Nat Rev Drug Discov. 2010; 9:615–627. [PubMed: 20616808]

10. Euliss LE, DuPont JA, Gratton S, DeSimone J. Imparting Size, Shape, and Composition Control of Materials for Nanomedicine. Chem Soc Rev. 2006; 35:1095–1104. [PubMed: 17057838]

11. Cheow WS, Chang MW, Hadinoto K. Antibacterial Efficacy of Inhalable Levofloxacin-Loaded Polymeric Nanoparticles against *E. coli* Biofilm Cells: the Effect of Antibiotic Release Profile. Pharm Res. 2010; 27:1597–1609. [PubMed: 20407918]

12. Wang AZ, Langer R, Farokhzad OC. Nanoparticle Delivery of Cancer Drugs. Annual Review of Medicine. 2012; 63:185–198.

13. Nederberg F, Zhang Y, Tan JP, Xu K, Wang H, Yang C, Gao S, Guo XD, Fukushima K, Li L, Hedrick JL, Yang YY. Biodegradable Nanostructures with Selective Lysis of Microbial Membranes. Nat Chem. 2011; 3:409–414. [PubMed: 21505501]

14. Moogooee M, Ramezanzadeh H, Jasoori S, Omidi Y, Davaran S. Synthesis and *In Vitro* Studies of Cross-Linked Hydrogel Nanoparticles Containing Amoxicillin. J Pharm Sci. 2010; 100:1057–1066. [PubMed: 21280053]

15. Pinto Alphandary H, Andremont A, Couvreur P. Targeted Delivery of Antibiotics Using Liposomes and Nanoparticles: Research and Applications. Int J Antimicrob Agents. 2000; 13:155–168. [PubMed: 10724019]

16. Italia JL, Sharp A, Carter KC, Warn P, Kumar MN. Peroral Amphotericin B Polymer Nanoparticles Lead to Comparable Or Superior *In Vivo* Antifungal Activity to that of Intravenous Ambisome or Fungizone. PLoS One. 2011; 6:e25744. [PubMed: 21998690]

17. Griffiths G, Nystrom B, Sable SB, Khuller GK. Nanobead-Based Interventions for the Treatment and Prevention of Tuberculosis. Nat Rev Microbiol. 2010; 8:827–834. [PubMed: 20938454]

18. Mohammadi G, Valizadeh H, Barzegar-Jalali M, Lotfipour F, Adibkia K, Milani M, Azhdarzadeh M, Kiafar F, Nokhodchi A. Development of Azithromycin-PLGA Nanoparticles: Physicochemical Characterization and Antibacterial Effect Against *Salmonella typhi*. Colloids Surf B Biointerfaces. 2010; 80:34–39. [PubMed: 20558048]

19. Maeda H. Tumor-Selective Delivery of Macromolecular Drugs Via the EPR Effect: Background and Future Prospects. Bioconjug Chem. 2010; 21:797–802. [PubMed: 20397686]

20. Kohanski MA, DePristo MA, Collins JJ. Sublethal Antibiotic Treatment Leads to Multidrug Resistance Via Radical-Induced Mutagenesis. Mol Cell. 2010; 37:311–320. [PubMed: 20159551]

21. Levy SB, Marshall B. Antibacterial Resistance Worldwide: Causes, Challenges and Responses. Nat Med. 2004; 10:S122–S129. [PubMed: 15577930]

22. Huh AJ, Kwon YJ. "Nanoantibiotics": A New Paradigm for Treating Infectious Diseases Using Nanomaterials in the Antibiotics Resistant Era. J Control Release. 2011; 156:128–145. [PubMed: 21763369]

23. Chung YC, Wang HL, Chen YM, Li SL. Effect of Abiotic Factors on the Antibacterial Activity of Chitosan Against Waterborne Pathogens. Bioresour Technol. 2003; 88:179–184. [PubMed: 12618038]

24. Lopez AI, Reins RY, McDermott AM, Trautner BW, Cai C. Antibacterial Activity and Cytotoxicity of PEGylated Poly(amidoamine) Dendrimers. Molecular BioSystems. 2009; 5:1148–1156. [PubMed: 19756304]

25. Wang J, Byrne JD, Napier ME, DeSimone JM. More Effective Nanomedicines Through Particle Design. Small. 2011; 7:1919–1931. [PubMed: 21695781]

26. He C, Hu Y, Yin L, Tang C, Yin C. Effects of Particle Size and Surface Charge on Cellular Uptake and Biodistribution of Polymeric Nanoparticles. Biomaterials. 2010; 31:3657–3666. [PubMed: 20138662]

27. Mercier RC, Stumpo C, Rybak MJ. Effect of Growth Phase and pH on the *In Vitro* Activity of a New Glycopeptide, Oritavancin (LY333328), Against *Staphylococcus aureus* and *Enterococcus faecium*. J Antimicrob Chemother. 2002; 50:19–24. [PubMed: 12096002]

28. Simmen HP, Battaglia H, Giovanoli P, Blaser J. Analysis of pH, pO2 and pCO2 in Drainage Fluid Allows for Rapid Detection of Infectious Complications During the Follow-Up Period After Abdominal Surgery. Infection. 1994; 22:386–389. [PubMed: 7698834]

29. Barrett, KE. Gastrointestinal Physiology. The McGraw Hill Companies, Inc.; 2006.

30. Barrett, KE.; Barman, SM.; Boitano, S.; Heddwen, B. Ganong's Review of Medical Physiology. 23 ed. 2010.

31. Fuchs S, Pane Farre J, Kohler C, Hecker M, Engelmann S. Anaerobic Gene Expression in *Staphylococcus aureus*. J Bacteriol. 2007; 189:4275–4289. [PubMed: 17384184]

32. Trevani AS, Andonegui G, Giordano M, Lopez DH, Gamberale R, Minucci F, Geffner JR. Extracellular Acidification Induces Human Neutrophil Activation. J Immunol. 1999; 162:4849–4857. [PubMed: 10202029]

33. Dubos RJ. The Micro-Environment of Inflammation of Metchnikoff Revisited. Lancet. 1955; 266:xxiv–5.

34. Simmen HP, Blaser J. Analysis of pH and pO2 in Abscesses, Peritoneal Fluid, and Drainage Fluid in the Presence or Absence of Bacterial Infection During and After Abdominal Surgery. Am J Surg. 1993; 166:24–27. [PubMed: 8328625]

35. Vermeulen M, Giordano M, Trevani AS, Sedlik C, Gamberale R, Fernandez-Calotti P, Salamone G, Raiden S, Sanjurjo J, Geffner JR. Acidosis Improves Uptake of Antigens and MHC Class I-Restricted Presentation by Dendritic Cells. J Immunol. 2004; 172:3196–3204. [PubMed: 14978127]

36. Tate S, MacGregor G, Davis M, Innes JA, Greening AP. Airways in Cystic Fibrosis are Acidified: Detection by Exhaled Breath Condensate. Thorax. 2002; 57:926–929. [PubMed: 12403872]

37. Poschet J, Perkett E, Deretic V. Hyperacidification in Cystic Fibrosis: Links with Lung Disease and New Prospects for Treatment. Trends Mol Med. 2002; 8:512–519. [PubMed: 12421684]

38. Tomb JF, White O, Kerlavage AR, Clayton RA, Sutton GG, Fleischmann RD, Ketchum KA, Klenk HP, Gill S, Dougherty BA, et al. The Complete Genome Sequence of the Gastric Pathogen *Helicobacter pylori*. Nature. 1997; 388:539–547. [PubMed: 9252185]

39. Simon, RH. Cystic Fibrosis: Antibiotic Therapy for Lung Disease. In: Basow, DS., editor. UpToDate. UpToDate; Waltham, MA: 2012.

40. Brooks, GF.; Carroll, KC.; Butel, JS.; Morse, SA.; Mietzner, TA. Jawetz, Melnick, & Adelberg's Medical Microbiology, 25th Edition. 25 ed. The McGraw-Hill Companies, Inc.; USA: 2010.

41. Fang B, Gon S, Park M, Kumar KN, Rotello VM, Nusslein K, Santore MM. Bacterial Adhesion on Hybrid Cationic Nanoparticle-Polymer Brush Surfaces: Ionic Strength Tunes Capture from Monovalent to Multivalent Binding. Colloids Surf B Biointerfaces. 2011; 87:109–115. [PubMed: 21640564]

42. Dillen K, Bridts C, Van der Veken P, Cos P, Vandervoort J, Augustyns K, Stevens W, Ludwig A. Adhesion of PLGA or Eudragit/PLGA Nanoparticles to Staphylococcus and Pseudomonas. Int J Pharm. 2008; 349:234–240. [PubMed: 17888598]

43. Hancock RE. Peptide Antibiotics. Lancet. 1997; 349:418–422. [PubMed: 9033483]

44. Liu L, Xu K, Wang H, Tan PK, Fan W, Venkatraman SS, Li L, Yang YY. Self-Assembled Cationic Peptide Nanoparticles as an Efficient Antimicrobial Agent. Nat Nanotechnol. 2009; 4:457–463. [PubMed: 19581900]

45. Vukomanovic M, Skapin SD, Jancar B, Maksin T, Ignjatovic N, Uskokovic V, Uskokovic D. Poly(D,L-lactide-co-glycolide)/Hydroxyapatite Core-Shell Nanospheres. Part 1: A Multifunctional System for Controlled Drug Delivery. Colloids Surf B Biointerfaces. 2011; 82:404–413. [PubMed: 20951005]

46. Misra R, Acharya S, Dilnawaz F, Sahoo SK. Sustained Antibacterial Activity of Doxycycline-Loaded Poly(D,L-lactide-co-glycolide) and Poly(epsilon-caprolactone) Nanoparticles. Nanomedicine (Lond). 2009; 4:519–530. [PubMed: 19572818]

47. Gref R, Minamitake Y, Peracchia MT, Trubetskoy V, Torchilin V, Langer R. Biodegradable Long-Circulating Polymeric Nanospheres. Science. 1994; 263:1600–1603. [PubMed: 8128245]

48. Lee ES, Na K, Bae YH. Polymeric Micelle for Tumor pH and Folate-Mediated Targeting. J Control Release. 2003; 91:103–113. [PubMed: 12932642]

49. Yin H, Lee ES, Kim D, Lee KH, Oh KT, Bae YH. Physicochemical Characteristics of pH-Sensitive Poly(L-histidine)-b-poly(ethylene glycol)/poly(L-lactide)-b-poly(ethylene glycol) Mixed Micelles. J Control Release. 2008; 126:130–138. [PubMed: 18187224]

50. Perez C, Sanchez A, Putnam D, Ting D, Langer R, Alonso MJ. Poly(lactic acid)-poly(ethylene glycol) Nanoparticles as New Carriers for the Delivery of Plasmid DNA. J Control Release. 2001; 75:211–224. [PubMed: 11451511]

51. Lambert RJ, Pearson J. Susceptibility Testing: Accurate and Reproducible Minimum Inhibitory Concentration (MIC) and Non-Inhibitory Concentration (NIC) Values. J Appl Microbiol. 2000; 88:784–790. [PubMed: 10792538]
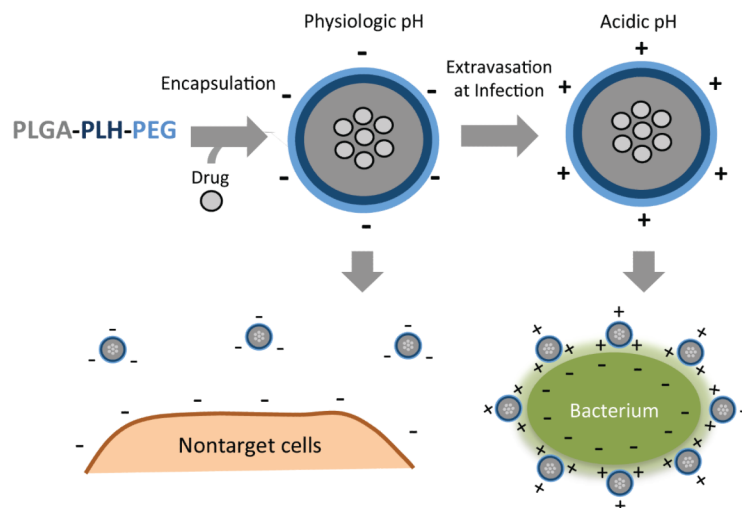
Figure 1.
Schematic representation of the designed nanoparticle (NP)-mediated drug targeting to bacterial cell walls. Drugs are encapsulated into NPs using a double emulsion/solvent evaporation process. The NPs avoid uptake or binding to nontarget cells or blood components at physiologic pH 7.4 due to a slight negative charge and surface PEGylation. Inflammation at a site of infection causes increased local vascular permeability, promoting NP extravasation. The weakly acidic conditions at sites of certain infections activate the surface charge-switching mechanism, resulting in NP binding to negatively charged bacteria. Finally, controlled release of the encapsulated drug leads to antibacterial effect.
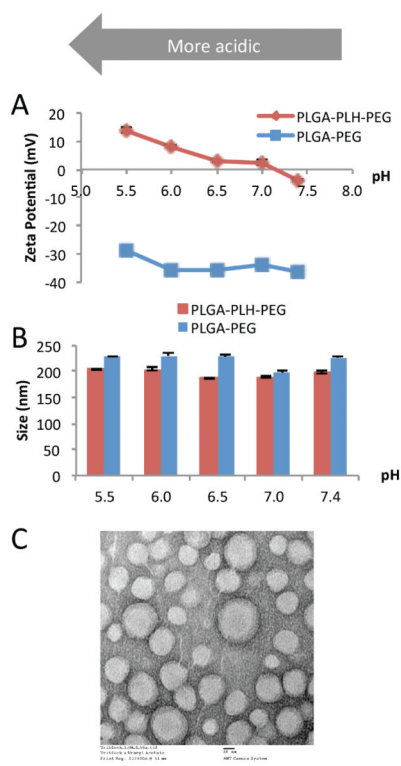
Figure 2.
Physicochemical characterization of NPs. (A) NP zeta potential vs pH demonstrates notable switching from anionic to cationic with decreases in pH in PLGA-PLH-PEG but not PLGA-PEG NPs. (B) NP size vs pH. (C) Transmission electron micrograph (TEM) of PLGA-PLH-PEG NPs. Scale bar 20 nm. N=3 for all observations.
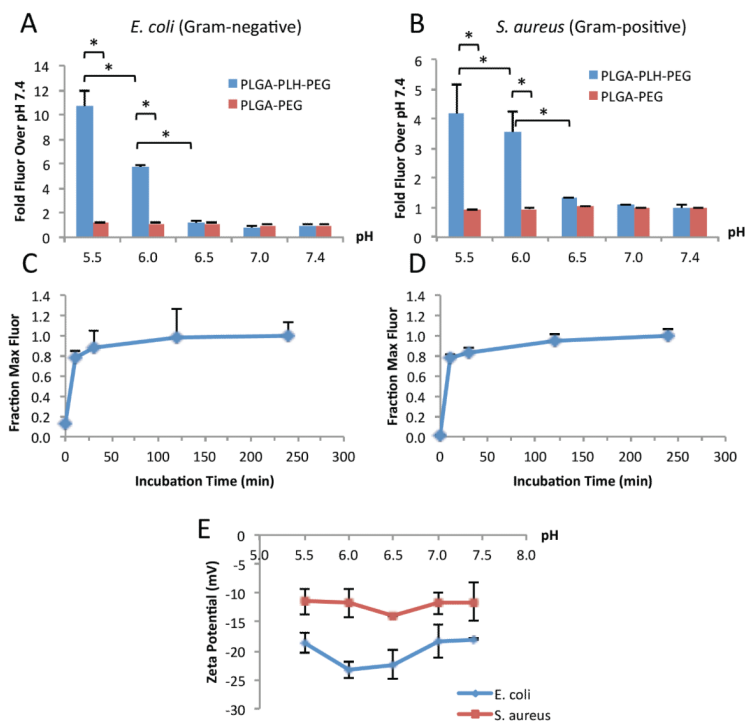
Figure 3.
NPs binding to representative bacteria. Alexa-488 labeled PLGA-PLH-PEG or PLGA-PEG NPs were incubated with (A) *E. coli* or (B) *S. aureus* in PBS at different pH levels ranging from 5.5 to 7.4; binding was assessed by flow cytometry and expressed as fold mean fluorescence over pH 7.4. (C) *E. coli* and (D) *S. aureus* binding kinetics studies at pH 6.0 show that bacterial binding occurs rapidly. (E) Zeta potential of bacteria with changes in pH. (* indicates $p < 0.05$). N=3 for all observations except in E, where N=2.
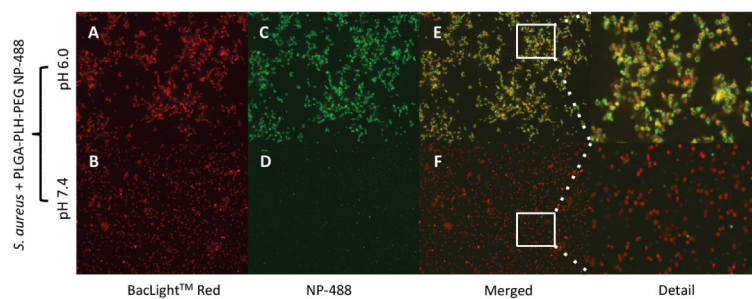
Figure 4.
Fluorescent confocal microscopy of pH-dependent binding. *S. aureus* bacteria labeled with *Bac*Light™ Red were treated with Alexa-488 labeled PLGA-PLH-PEG NP-488 at pH 6.0 (panels A, C, E) or pH 7.4 (panels B, D, F). (A, B) *Bac*Light™ Red (C, D) NP-488 (E, F) Merge of *Bac*Light™ Red and NP-488, with yellow indicating co-localization. The white box in E, F demonstrates a detail of the merged image, showing the bacterial cell wall-associated NP-488 at pH 6.0 but not pH 7.4.
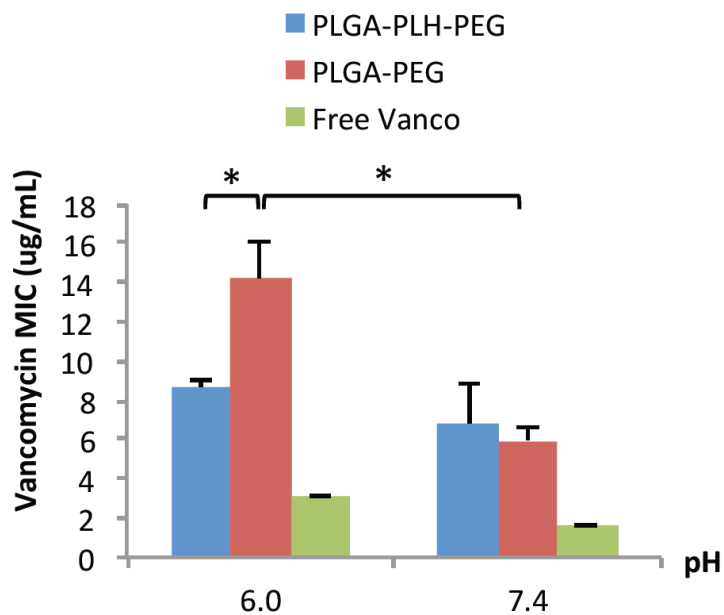
Figure 5.
NP-mediated vancomycin delivery to *S. aureus*. Minimum inhibitory concentrations (MIC) determined from microplate broth dilution assays at pH 6.0 or 7.4, demonstrating loss of drug activity in PLGA-PEG[Vanco] and free vancomycin but not PLGA-PLH-PEG[Vanco]. (* indicates p < 0.05).

Table 1

Minimum bactericidal concentration (MBC) at pH 6.0 and pH 7.4 in *S. aureus*

		Min. Bactericidal Conc. (MBC)	
Treatment	pH	[NP] (ug/mL)	[Vanco] (ug/mL)
PLGA-PLH-PEG [Vanco]	6.0	250	20
PLGA-PLH-PEG [Vanco]	7.4	250	20
PLGA-PEG [Vanco]	6.0	500	40
PLGA-PEG [Vanco]	7.4	250	20
Free Vanco	6.0	N/A	6
Free Vanco	7.4	N/A	3
PLGA-PLH-PEG	6.0	> 500	N/A
PLGA-PLH-PEG	7.4	> 500	N/A
PLGA-PEG	6.0	> 500	N/A
PLGA-PEG	7.4	> 500	N/A